Selected for the *International Journal of Thermophysics*

The influence of modern, low emissive coatings on the coupled heat and mass transfer of envelope parts of building[1]

Peter Häupl[2], Horst Stopp[3]; Peter Strangfeld[3]

---

[1] Paper presented at the Fourteenth Symposium on Thermophysical Properties, June 25-30 2000, Boulder, Colorado, U.S.A.

[2] Technical University of Dresden, Institut für Bauklimatik, D-01062 Dresden, Germany

[3] University of Applied Science Lausitz, Building Physics, PF 130268, D-03042 Cottbus, Germany

ABSTRACT

At present in some European countries and overseas is discussed the effectivness of infrared reflecting coatings on the heat transmission of envelope parts of buildings.The situation seems to be clear and is used as commercial propagation. By the reduction of the longwave emission coefficient the surface temperatures of facades are influenced in a favourable way. During wintertime the temperature at an external surface is raised and by that the heat losses are diminished up to 20%. With regard to the utililization of the solar radiation a selected emission coeffecient must be presupposed. But all the announcements of a diminished energy consumption neglect the moisture influence. By driving rain, moisture moving, water vapour diffusion and condensation a coupled heat and mass transfer takes place. Measurments are in progress and the processes have been investigated by a comprehensive modelling and numerical simulation depend on:

- the climate boundary conditions both indoor and outdoor by using different TRY including all time depending climate components
- the structures of outside walls and roofs with regard to their thermal resistance and the sequence of layers
- the thermal hygric material properties such as the emission coefficient, water capillary activity of the rendering, water vapor diffusion resistance and so on.

The results concerning energy consumption during the heating period and cooling effect including the moisture content and its distribution and the problems of condensation are demonstrated and discussed in comparison with standard coatings.

KEY WORDS: building physics, coupled heat/moisture transfer, envelope parts of buildings, longwave emission, numerical simulation.

1 INTRODUCTION

The current situation of the building physics is characterized by looking for energy saving. In most cases the requirements are related to the heat transmission. This means the so-called U-value must be reduced with regard to the former envelope parts of buildings.This is easily to fulfill by a greater thickness of the insulation layer or materials with a lower thermal conductivity. But by the climate conditions in reality dry structures are very seldom and we have to consider the moisture transfer, caused by condensation, driving rain and built in moisture [1]. The better the thermal insulation and the air tightness the more the effects of moisture are evident and can be the reason of damages.

On the other hand there could be an improvement of the energy balance by the reduction of the longwave radiation at the surfaces. Admittedly in this investigations the condensation and distribution of moisture is to consider also, if the results of calculation shall be realistic. Therefore the material properties of the coupled heat and mass transfer are taken into account for the numerical simulation of the effects of radiation. Besides the emissivity of surfaces and the thermal properties the material functions for the capillary water conduction [2], the water vapor transfer and the sorptionisotherm are used under the climatic boundary conditions of a TRY for middle Europe.

The calculations are carried out by means of a computercode [3], basing on a comprehensive modeling of the coupled heat, air and moisture transport and validated by the Int. Energy Agency, Annex 24 (heat, air and moisture transfer in insulated envelope parts) [4].

2 INVESTIGATED STRUCTURES AND MATERIAL PROPERTIES

In order to find out the different influences to the maximum effect of the longwave

radiation the arrangement and the properties of the multilayered constructions are varied, listed from the inside to the outside as follows:

Wall 1		internal plastering	brick masonry	external rendering
Thickness s	mm	15	240	20
Thermal conductivity λ_0	$W \cdot m^{-1} \cdot K^{-1}$	1.0	0.8	1.05
Moisture coeff. $d\lambda/dw$	$W \cdot m^{-1} \cdot K^{-1}/V\%$	$4.35 \cdot 10^{-2}$	$3.16 \cdot 10^{-2}$	$4.35 \cdot 10^{-2}$
Mass density ρ	$kg \cdot m^{-3}$	1470	1720	1470
Specific heat capacity c :	$J \cdot kg^{-1} \cdot K^{-1}$	850	920	850
Max. capillary conductivity a_o	$m^2 \cdot s^{-1}$	$1.0 \cdot 10^{-9}$	$3.0 \cdot 10^{-7}$	$1.0 \cdot 10^{-9}$
Parameter capill.conduct. function k		0.7	0.2	0.7
Max. hygroscopic value w_h	V%	3	1.5	3
Saturation moisture w_s	V%	24	34	24
Vapor diffusion resistance factor μ		21	10	21
Absorption coeff. for solar rad. a	-	-	-	0.6

Wall 2		internal plastering	brick masonry	external rendering
Thickness s	mm	15	240	20
Thermal conductivity λ_0	$W \cdot m^{-1} \cdot K^{-1}$	1.0	0.5	1.05
Moisture coeff. $d\lambda/dw$	$W \cdot m^{-1} \cdot K^{-1}/V\%$	$4.35 \cdot 10^{-2}$	$3.16 \cdot 10^{-2}$	$4.35 \cdot 10^{-2}$
Mass density ρ	$kg \cdot m^{-3}$	1470	1000	1470
Specific heat capacity c :	$J \cdot kg^{-1} \cdot K^{-1}$	850	920	850
Max. capillary conductivity a_o	$m^2 \cdot s^{-1}$	$1.0 \cdot 10^{-9}$	$1.0 \cdot 10^{-8}$	$1.0 \cdot 10^{-9}$
Parameter capill.conduct. function k	-	0.7	0.2	0.7
Max. hygroscopic value w_h	V%	3	7	3
Saturation moisture w_s	V%	24	30	24
Vapor diffusion resistance factor μ	-	21	10	21
Absorption coeff. for solar rad. a	-	-	-	0.6

Wall 3		Gypsum board	Insula-tion	Adhesive	internal plastering	brick masonry	External rendering
s	mm	13	60	2	15	240	20
λ_0	$W \cdot m^{-1} \cdot K^{-1}$	0.21	0.043	1.34	1.0	0.8	1.05
$d\lambda/dw$	$W \cdot m^{-1} \cdot K^{-1}/V\%$	$1.88 \cdot 10^{-2}$	$4.35 \cdot 10^{-2}$	$4.35 \cdot 10^{-2}$	$4.35 \cdot 10^{-2}$	$3.16 \cdot 10^{-2}$	$4.35 \cdot 10^{-2}$
ρ	$kg \cdot m^{-3}$	900	115	1500	1470	1720	1470
c	$J \cdot kg^{-1} \cdot K^{-1}$	850	850	1000	850	920	850
a_o	$m^2 \cdot s^{-1}$	$1.0 \cdot 10^{-5}$	$2.0 \cdot 10^{-9}$	$1.25 \cdot 10^{-11}$	$1.0 \cdot 10^{-9}$	$3.0 \cdot 10^{-7}$	$1.0 \cdot 10^{-11}$
k	-	0.2	1.25	0.25	0.7	0.2	0.7
w_h	V%	2	1.5	4	3	1.5	3
w_s	V%	65	16	20	24	34	24
μ	-	8	3.4	4	21	10	21
a	-	-	-	-	-	-	0.6

Walls 4 and 5, 6

The wall variations number four corresponds with wall 1 exepted by the max. capillary conductivity of the external rendering ($a_0 = 1.0 \cdot 10^{-11}$ $m^2 \cdot s^{-1}$).

The walls 5 and 6 differ from number 3 and 4 by a larger thickness of the original masonry: s=365 mm.

Roof 1		bearing structure: gas concrete	waterproof. layer
Thickness s	mm	300	6
Thermal conductivity λ_0	$W \cdot m^{-1} \cdot K^{-1}$	0.16	0.15
Moisture coeff. $d\lambda/dw$	$W \cdot m^{-1} \cdot K^{-1}/V\%$	$1.38 \cdot 10^{-2}$	$1.16 \cdot 10^{-2}$
Mass density ρ	$kg.m^{-3}$	600	1200
Specific heat capacity c :	$J \cdot kg^{-1} \cdot K^{-1}$	1050	840
Max. capillary conductivity a_o	$m^2 \cdot s^{-1}$	$5.0 \cdot 10^{-9}$	$1.0 \cdot 10^{-20}$
Parameter capill.conduct. function k	-	1.25	0.2

Max. hygroscopic value w_h	V%	4	0.001
Saturation moisture w_s	V%	65	0.02
Vapor diffusion resistance factor μ	-	7	10000
Absorption coeff. for solar rad. a	-	-	0.6

3 COMPUTERCODE DIM

The used program variation DIM 3.1 bases on own researches of the group [5]. Since the 80ties the modeling of the heat, air, and moisture transport including the measurements of hygrothermal parameter of materials was developed and computerized [6]. Many investigations demonstrate the performance of DIM. In-situ measurements were carried out to verify the code. For instance in connection with the restoration of worth preserving facades moisture and temperature fields were investigated. Fig.1 shows the comparison between measured and and calculated course of the temperature and humidity within an internal insulated outside wall [7].

4 RESULTS OF NUMERICAL SIMULATION

The following principle sketch demonstrates the complex process: enthalpie, energy and mass transfer by vapor-, capillary water transport and phase changes due to the driving rain, condensation and water vapor-, temperature- and moisture gradients. In order to demonstrate the maximum of the effects the coatings of structures with a few evaporation cooling (no capillary active rendering) and no longwave emission (ε=0) are compared in opposite to coatings with a large evaporation cooling (max. of its capillary conductivity $a_o \geq 10^{-9} m^2/s$) and a maximum of the longwave emission (ε = 0.9).

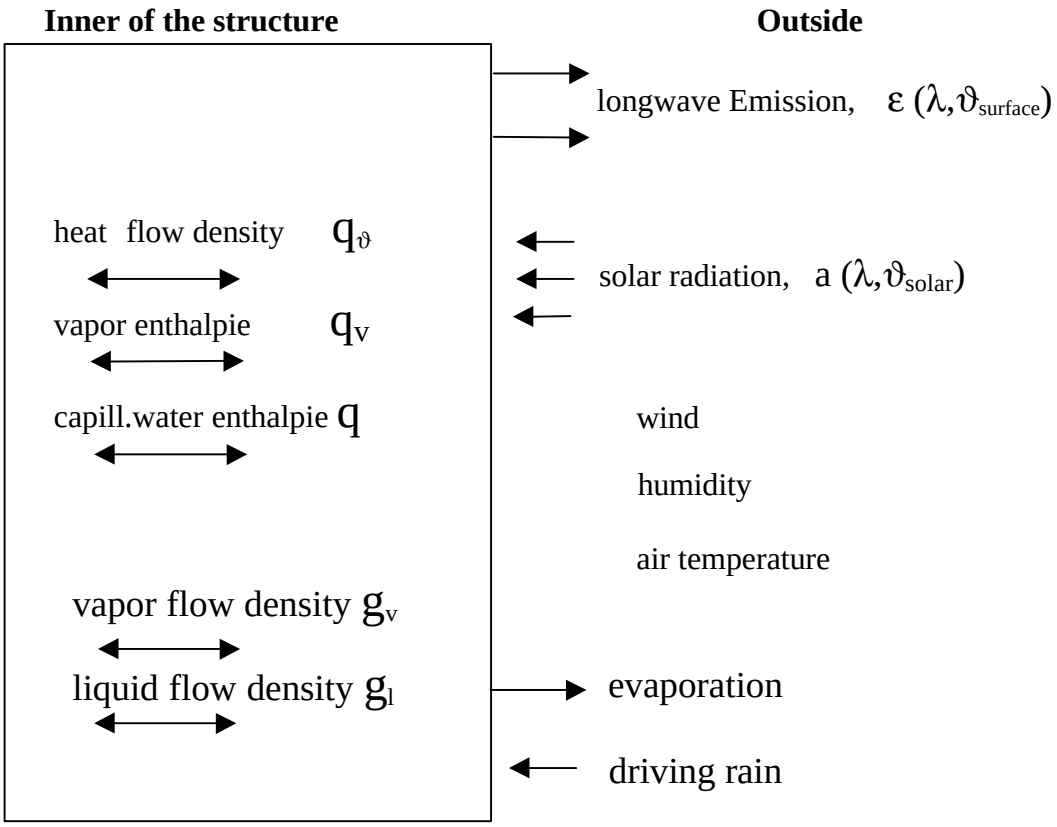

4.1 External walls 1, 2

The simple masonry walls1 and 2 are characterized by a capillary activ rendering. Fig. 2 shows the influence of the hygrothermal parameters to the total hygroscopic and overhygroscopic moisture content of these two simple western directed masonry walls and the difference of its moisture , caused by no capillary activ coatings. In all cases the longwave emission coefficient ε = 0. Within a masonry with an usual capillary activ rendering the total moisture content varies yearly around 4 kg/m^2, reduced to less than 0.5 kg/m^2 by an waterproofing coating. The average value of total moisture decreases from 13.5 kg/m^2 to 8 kg/m^2 (hygroscopic material, w_h=7V%) and from 6 kg/m^2 to 2 kg/m^2 (low-hygroscopic material, w_h=3V%) respectively by such special coatings.

The influence of the point of compass is investigated also. In fig.3 the total moisture content of western or southern directed walls (wall no. 1) with water proofing coatings are compared. This means the evaporation cooling effect can be neglected. In the case of usual longwave emission (ε=0.9) the difference of the total moisture content is less than 0.1 kg/m^2. The difference between a longwave emissive and an infrared reflecting south directed wall is few too, only about 0.2kg/m^2.

The less the penetration of driving rain and the less the moisture content the better the thermal insulation. This means a drop of the temperatures at the external surface of outside walls during winter time and a diminishing of the heat transmission. On the other hand the surface temperature raises owing to a reduced longwave emission and evaporation cooling.

The fig. 4 and fig. 5 quantify these effects. For the walls 1 and 2 the fig.4 shows the differences of the external surface temperatures up to 3 K for the Middle Europe climate. The effective U-value of the fig. 5 represents the heat flow density at the internal surface of the building envelope related to the total air temperature difference between indoor and outdoor during the heating period. The worst case is characterized by a surface with an usual emission coefficient $\varepsilon \approx 0.9$ and a large evaporation cooling. Fig.5 demonstrates, that the effects of moisture of outside walls are in the same magnitude as the effect of a reduction of emission. The theoretical total maximum could be about 15 %.

The better the insulation the larger the relative effects. In case of the 240mm wall structure with a thermal conductivity of 0.5 W/m·K the reduction of the evaporation cooling effect is 10% instead of 7% and the total maximum of a theoretical improvement (ε= 0) increases up to 17%.

4.2 External wall 3

It follows an internal insulated brick masonry wall (wall no.3) with a limited capillary activ external rendering. Fig.6 represents the moisture field in course of 5 years, if the wall is improved by an internal insulation due to worth preserving facade. The fluctuation of moisture at the external surface by driving rain and the yearly condensation at the cold side of the thermal insulation layer during winter period is to recognize very well.

The figures 7 and 8 demonstrate the effect of the reduced emission on the inner of the internal insulated outside wall 3. Due to the increased temperature up to 2K at the cold side of the insulation layer caused by no longwave emission (fig.7) the relative humidity decreases at the same place up to 10% (fig.8).

4.3 External walls 3,4 and 5,6

In fig. 9 the results of the walls 3 and 4 (thickness 240 mm) are compared to the results for the walls 5 and 6 with a thickness of 365 mm, all walls are covered with a moderate capillary activ external rendering. There is no difference between unisolated and internal isolated outside wall structures independent on their thicknesses with regard to the relative effects of a reduced emission.

4.4 Flat roof 1

On the one hand the evaporation cooling effect is reduced by the capillary inactiv waterproof membrane, on the other hand the influence of the longwave radiation increases due to the emission to the whole hemisphere. Fig.10 represents the course of the heat flow density at the inside of the roof construction. The energy saving by an infrared reflecting coating is more than 10%.

Fig. 11 shows the time depending temperatures at the interior surface (harmonic oscillation of the room temperature), at the skin of the roof and in a distance of 100 mm

from that. The moderate values during sommer time are caused by an moderate absorption coefficient of 0.6.

5 SUMMARIZING

Up to now it is very difficult to produce a total infrared reflecting coating for building envelopes and above all things to protect against dusting and pollution. So the results above are maximum effects but by them it is possible to evaluate the measures and costs with regard to an energy saving. The effects depend on the envelope part. Under the climate boundary conditions of Middle Europe for outside walls with a thermal resistance up to 1.0 $m^2 \cdot K/W$ the maximum of the effect by a reduction of the longwave emission could be about 10% and is in the same magnitude as the effect of moisture influences. For flat roofs the longwave radiation effect on the heat transmission transport could reach 15%.

6 REFERENCES

[1] Fechner,H.; Häupl,P.; Stopp,H.; Strangfeld,P. Measurements and numerical simulation of the heat and moisture transfer in envelope parts of buildings. Proceedings of the Int. Conference on TPPM99, Singapore, (1999).

[2] Plagge,R.; Grunewald,J.; Häupl,P. Simultaneous determination of water retention characteristic and moisture conductivity using instantaneous profile techniques. Proceedings of the 10. Bauklimatisches Symposium, pp.433-444, TU Dresden, (1999).

[3] Grunewald,J.; Plagge,R. Full documentation of the numerical simulation program DIM3.1. Vol. 5 of the final report of the Brite-Euram Project BRPR-96-0229: Developement of a new methdology to analyse the durability of facade repair and retrofitting systems. TU Dresden, Germany, (1999).

[4] Hens,H. IEA-Annex 24: Final report, Vol.1,Task Modelling, K.U.-Leuven, (1996).

[5] Häupl,P.; Fechner,H.; Stopp,H. Coupled heat air and moisture transfer in building structures. Int.J. Heat Mass Transfer, Vol.40 No 7, pp.1633-1642, (1997).

[6] Häupl,P.; Stopp,H. Feuchtetransport in Baustoffen und Bauwerksteilen. Habilitations schrift, Vol. 1 – 5, Techn. Univ. Dressden, (1987).

[7] Fechner,H.; Häupl,P.; Stopp,H. Thermische Sanierung eines Gründerzeithauses mit einer kapillaraktiven Calciumsilikatinnendämmung. WTA-Schriftenreihe, H.18, 51-68, Freiburg, (1999).

Figure Captions

Fig.1 Comparison of measured values of the temperature / relative humidity and numerical simulated results by means of the computercode DIM between internal insulation and plaster of a brick masonry wall.

Fig.2 Total moisture content dependent on hygroscopicity and capillary water conductivity, TRY Essen, (walls1,2).

Fig.3 Total moisture content of western and southern directed external walls, coated, TRY Essen, (wall 1).

Fig.4 Surface temperatures at the west wall dependent on different coatings (wall 1,2), TRY Essen.

Fig.5 Effectiv U-values dependent on structures, coatings and longwave emission (wall 1,2).

Fig.6 Moisture field of an internal insulated brick masonry wall, TRY Essen (wall 3).

Fig.7 Course of temperature at the cold side of the insulation layer of the construction fig.6

Fig.8 Course of relative humidity at the cold side of the insulation layer of the construction fig.6

Fig.9 Effect of longwave emission regarding effectiv U-value dependent on thickness and insulation of western directed external walls, TRY Essen, (walls 4,5 and 6,7).

Fig.10 Heat flow density at the internal surface of a gas concrete flat roof structure, TRY Essen (roof 1).

Fig.11 Course of temperature within and at the surface of a gas concrete flat roof structure, TRY Essen (roof 1).

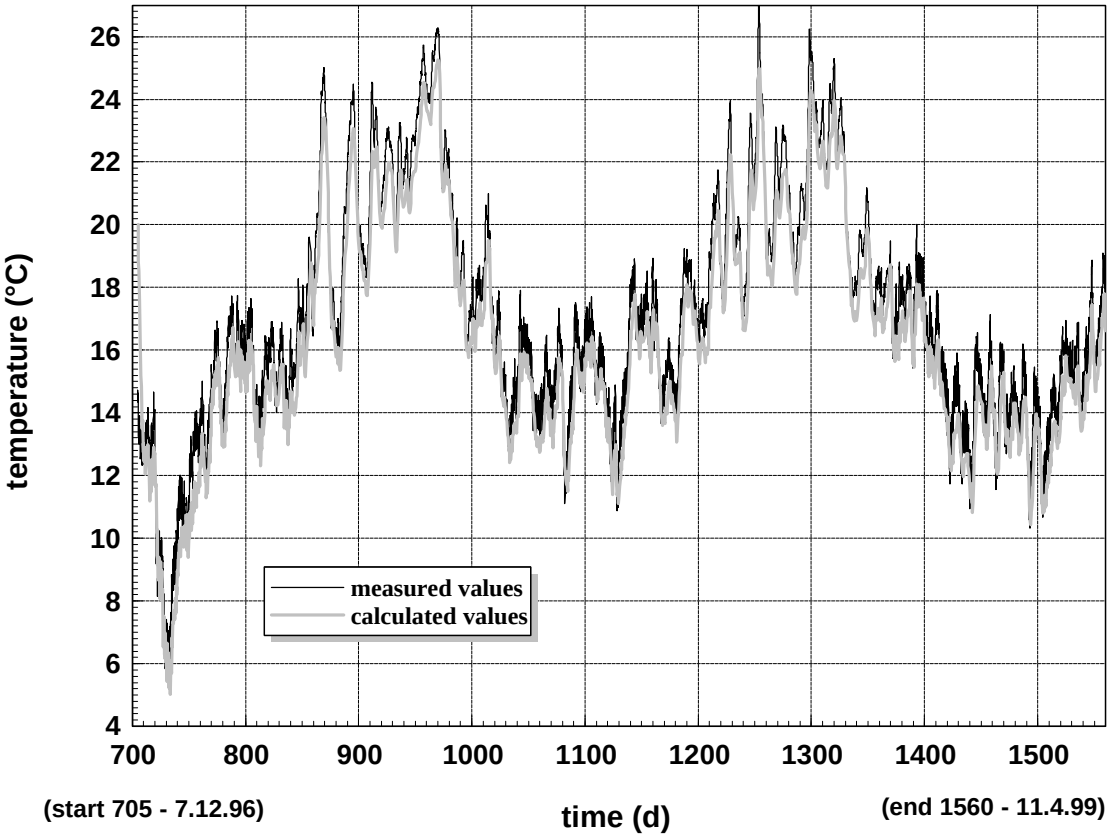

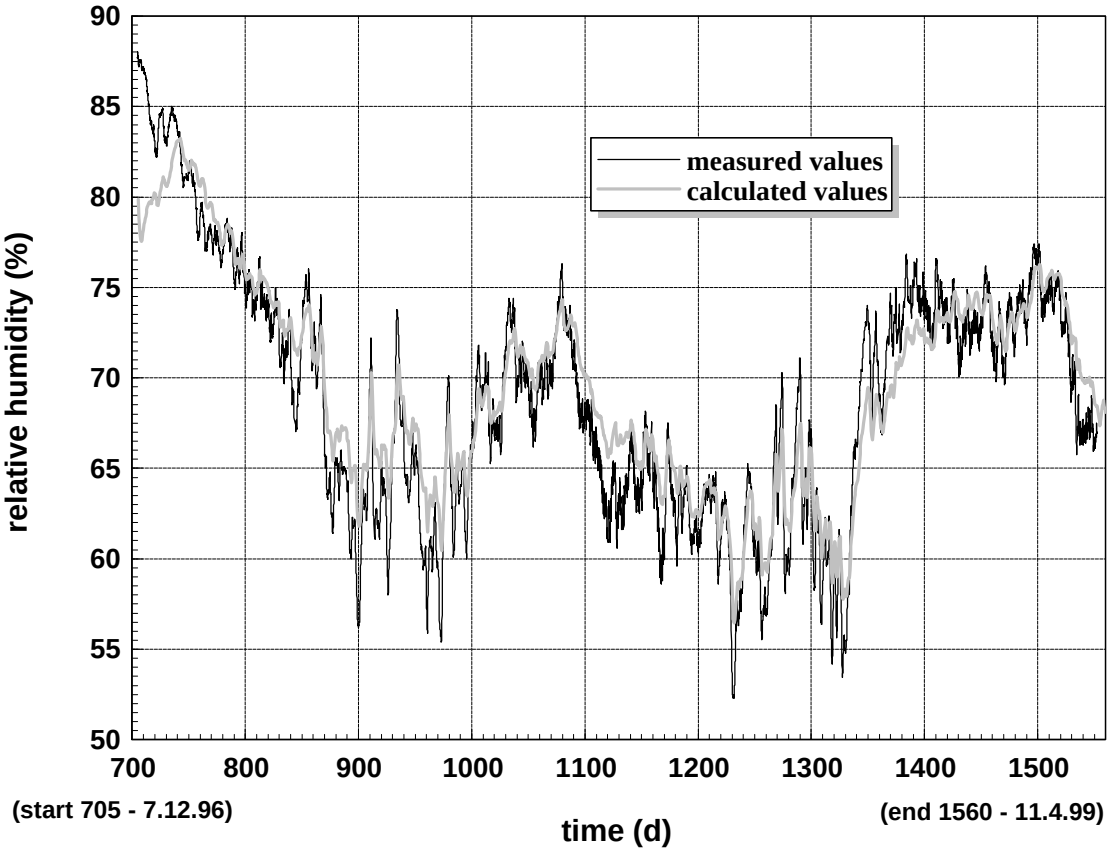

Fig.1 Comparison of measured values of the temperature / relative humidity and numerical simulated results by means of the computercode DIM between internal insulation and plaster of a brick masonry wall.

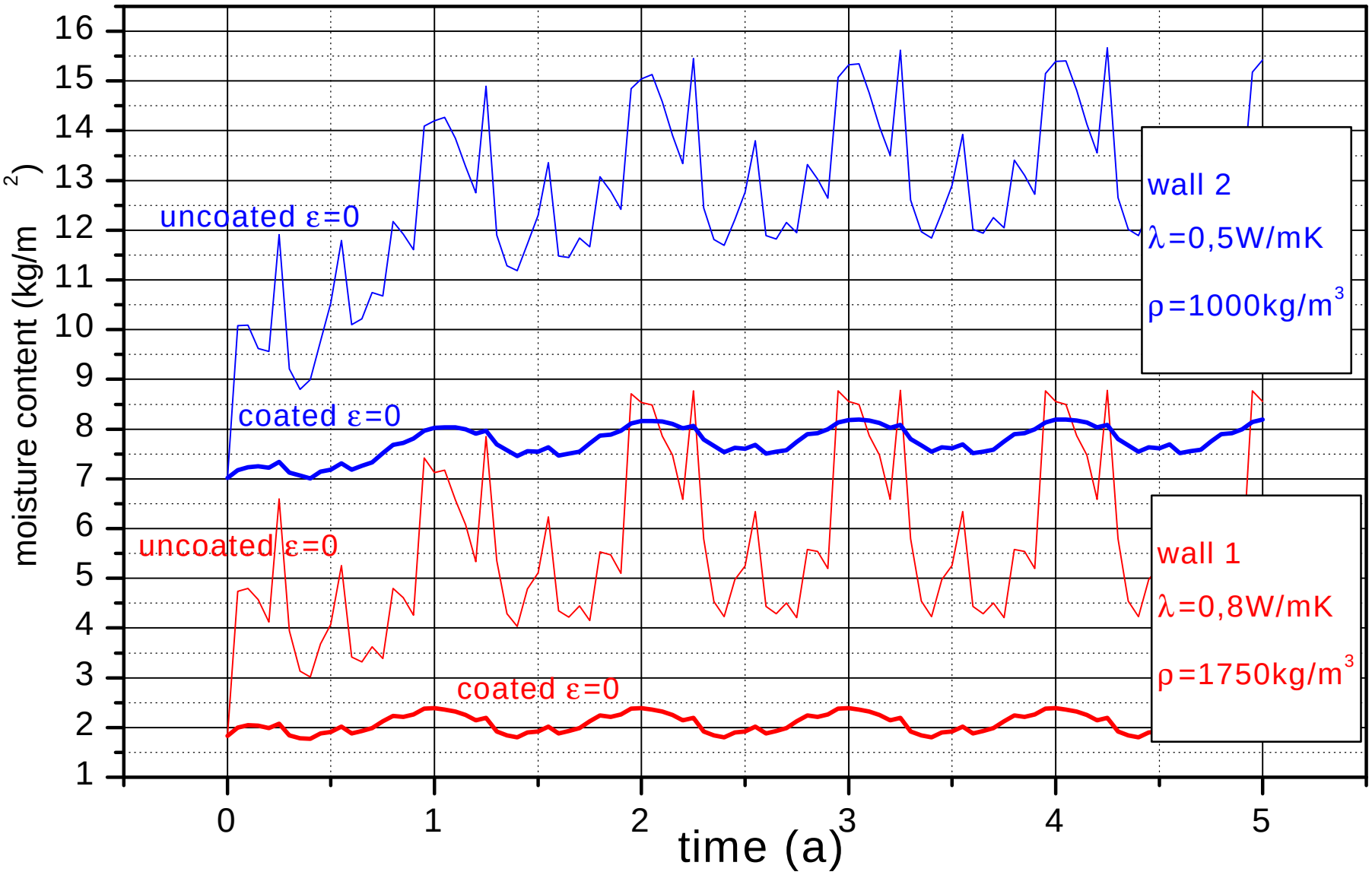

Fig.2 Total moisture content dependent on hygroscopicity and capillary water conductivity, TRY Essen, (walls1,2).

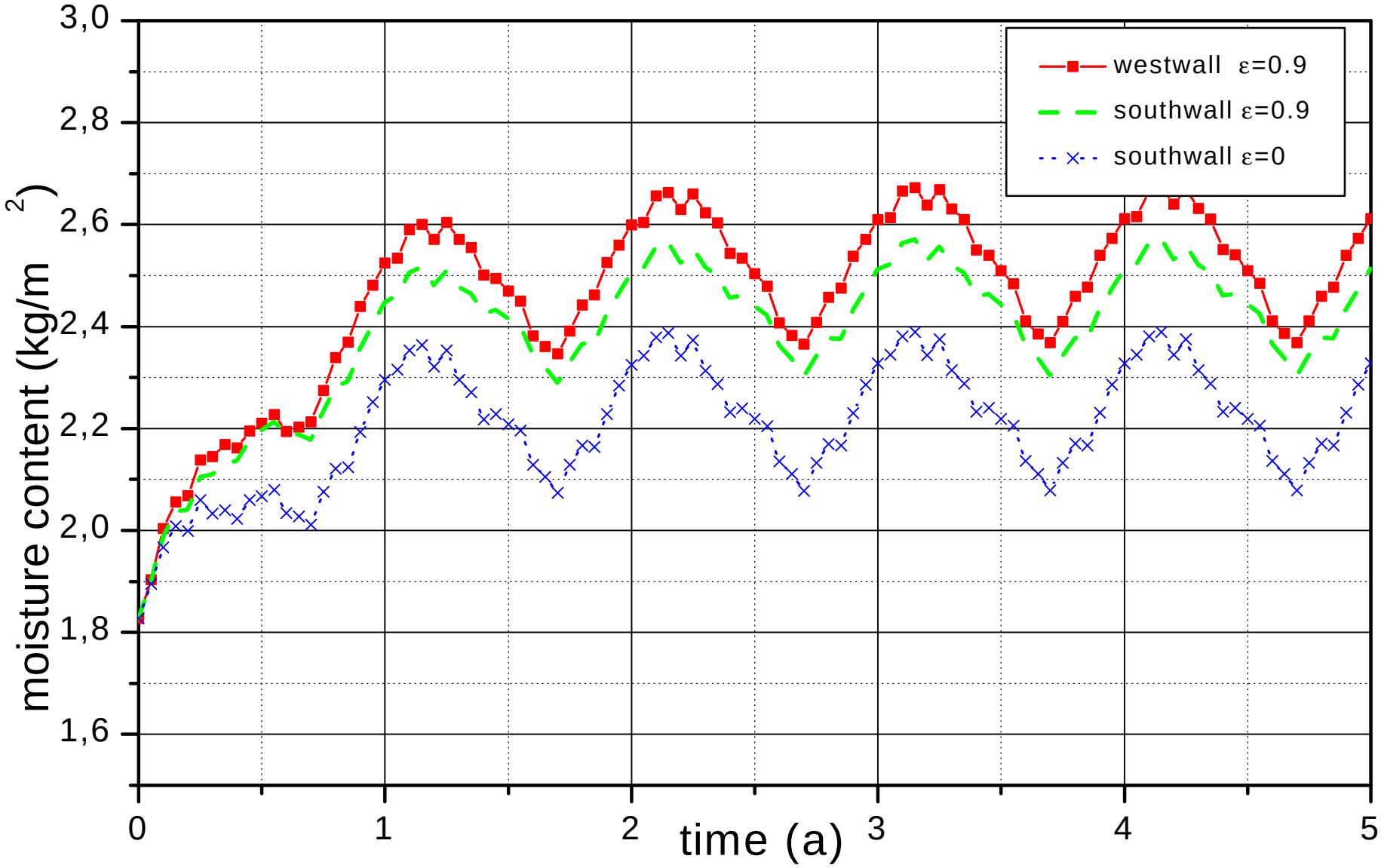

Fig.3 Total moisture content of western and southern directed external walls, coated, TRY Essen (wall 1).

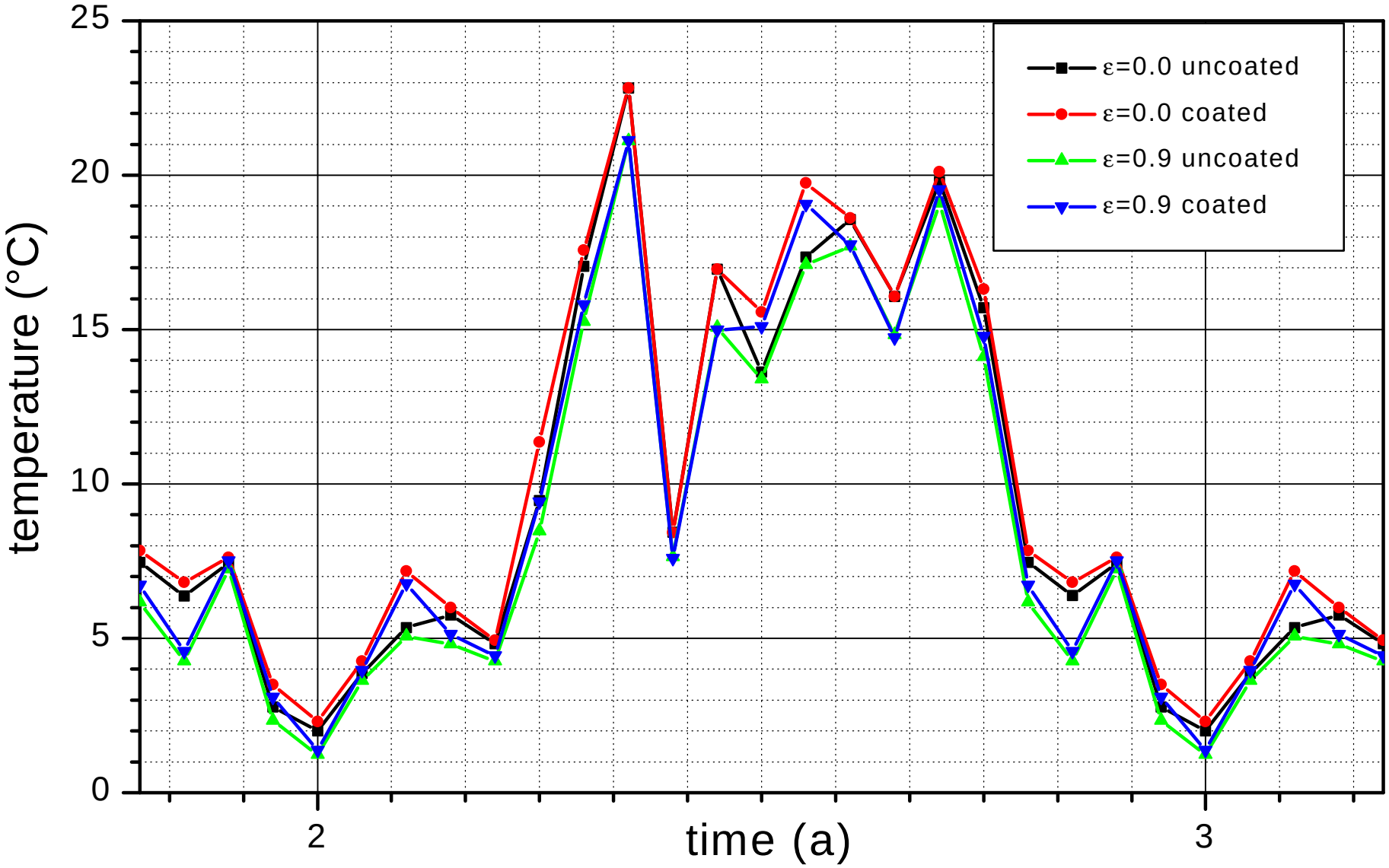

Fig.4 Surface temperatures at the west wall dependent on different coatings (wall 1,2), TRY Essen.

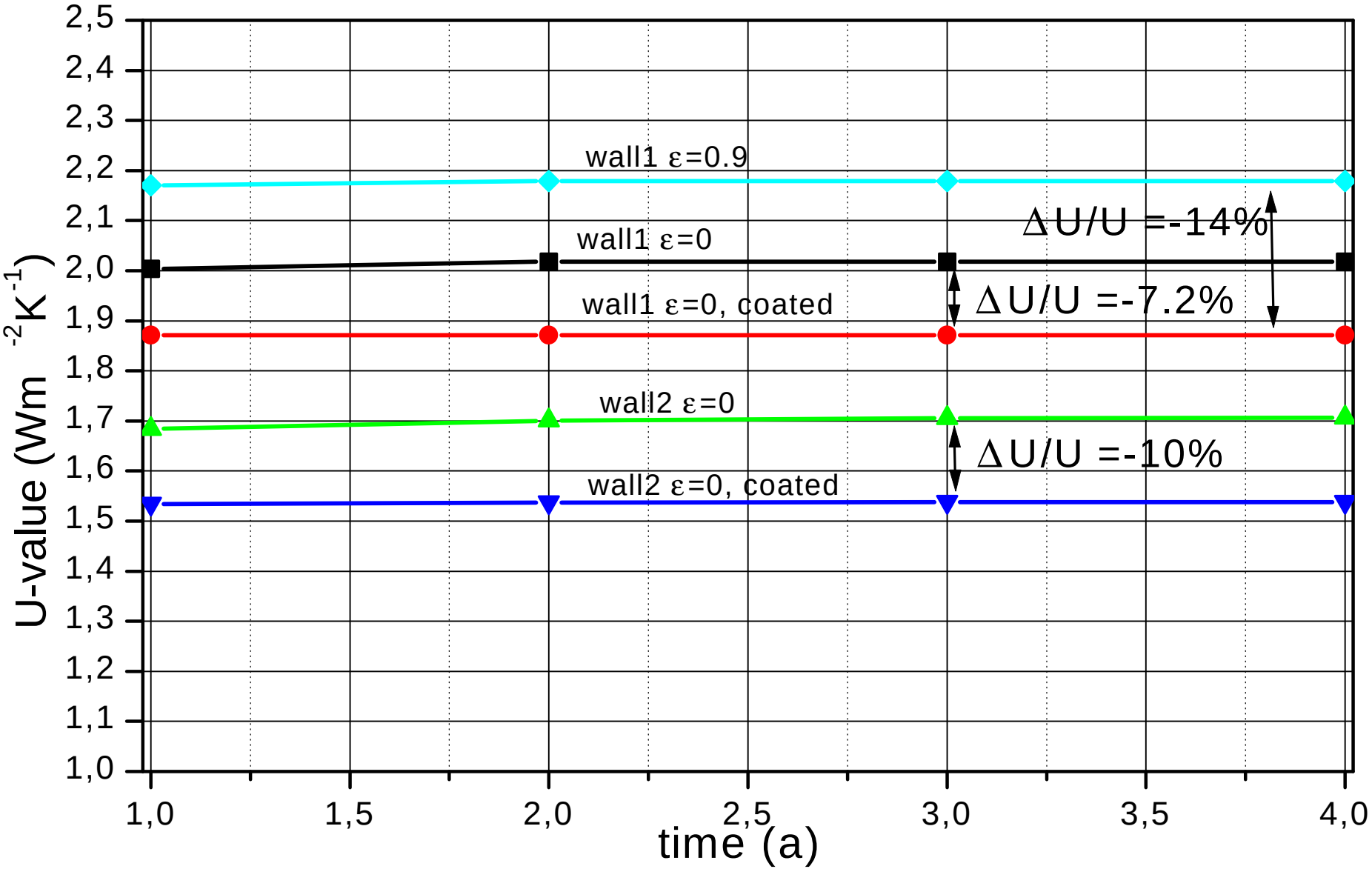

Fig.5 Effectiv U-values dependent on structures, coatings and longwave emission (wall 1,2).

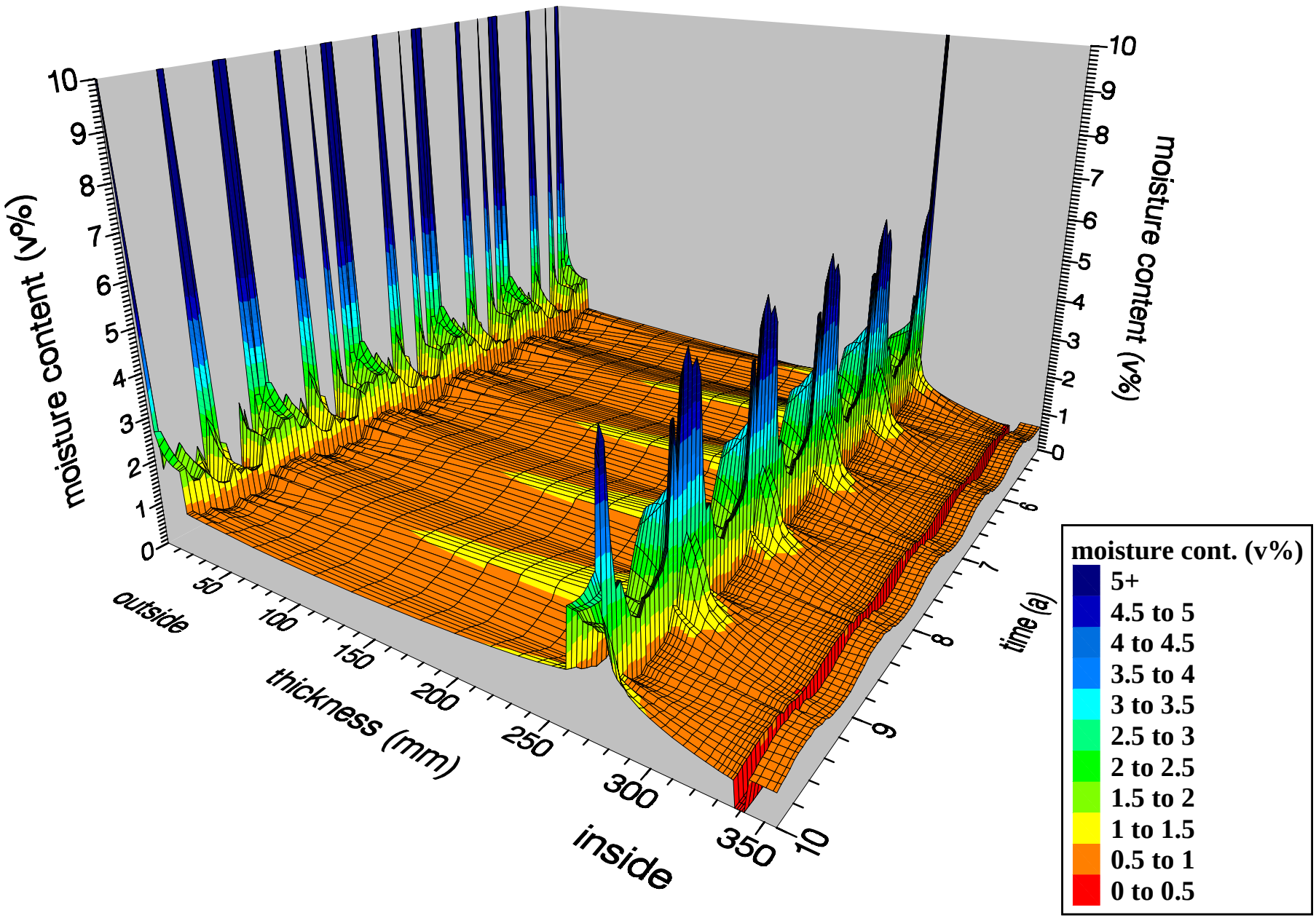

Fig.6 Moisture field of an internal insulated brick masonry wall, TRY Essen (wall 3).

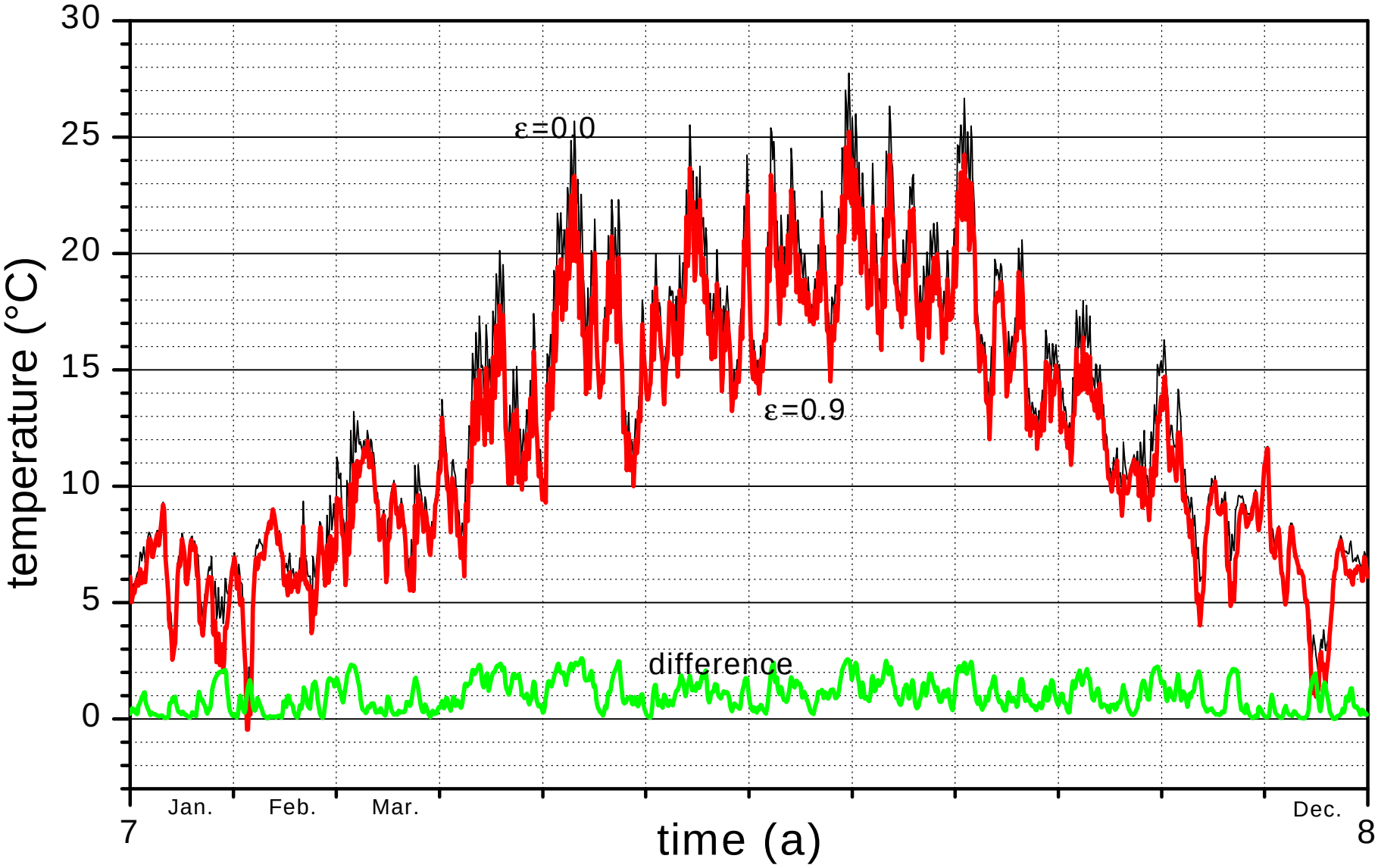

Fig.7 Course of temperature at the cold side of the insulation layer of the construction fig.6

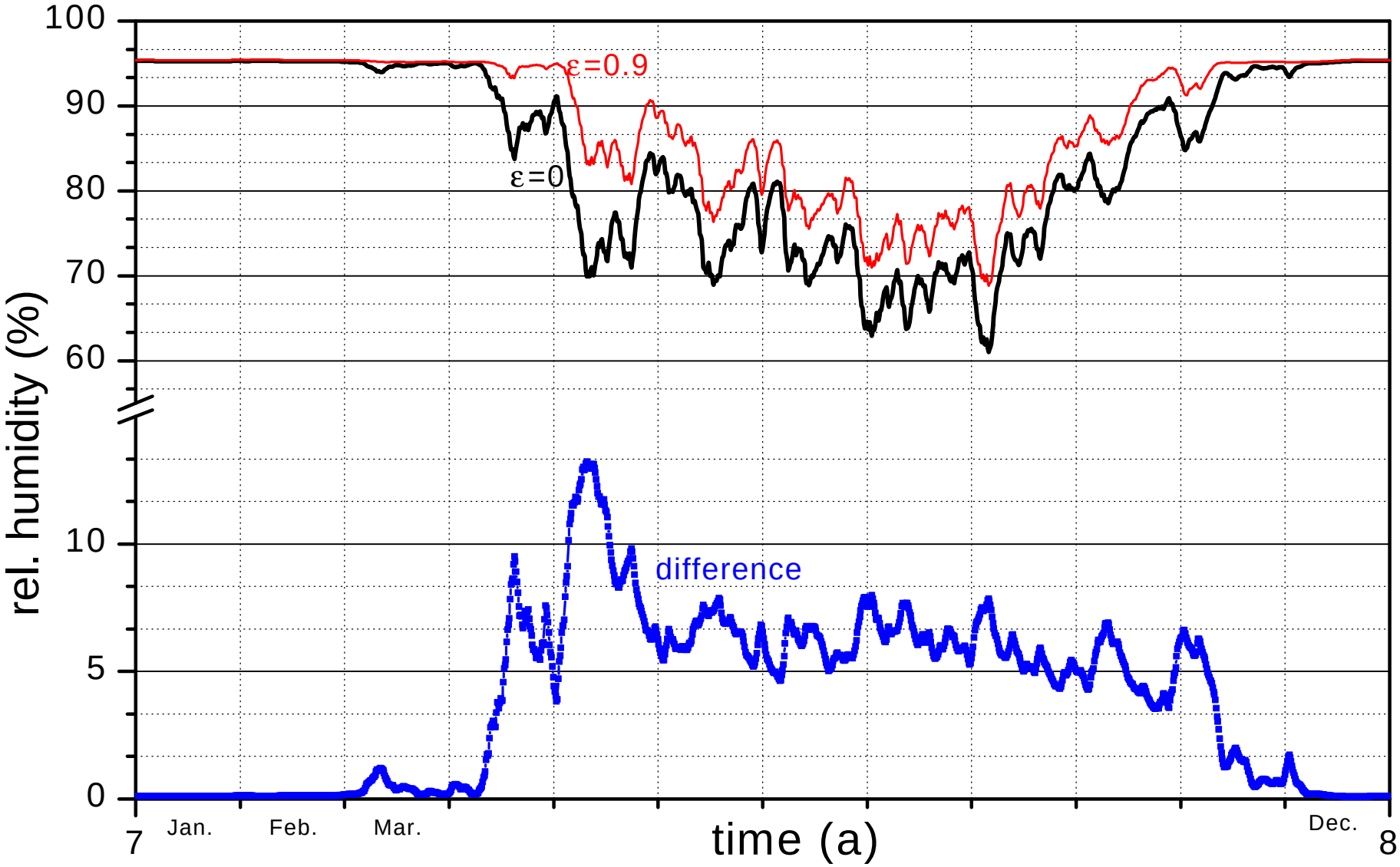

Fig.8 Course of relative humidity at the cold side of the insulation layer of the construction fig.6

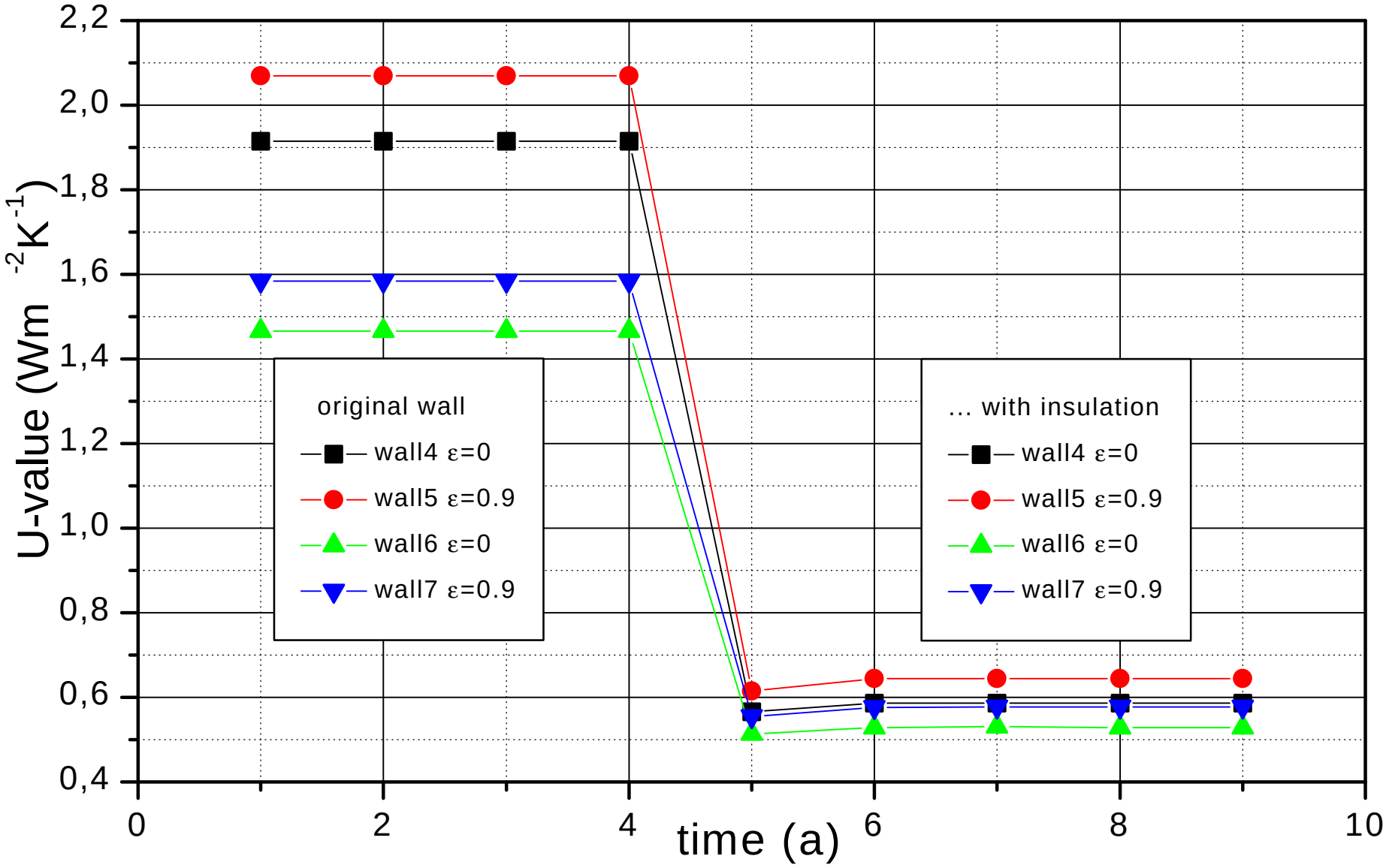

Fig.9 Effect of longwave emission regarding effectiv U-value dependent on thickness and insulation of western directed external walls, TRY Essen, (walls 4,5 and 6,7).

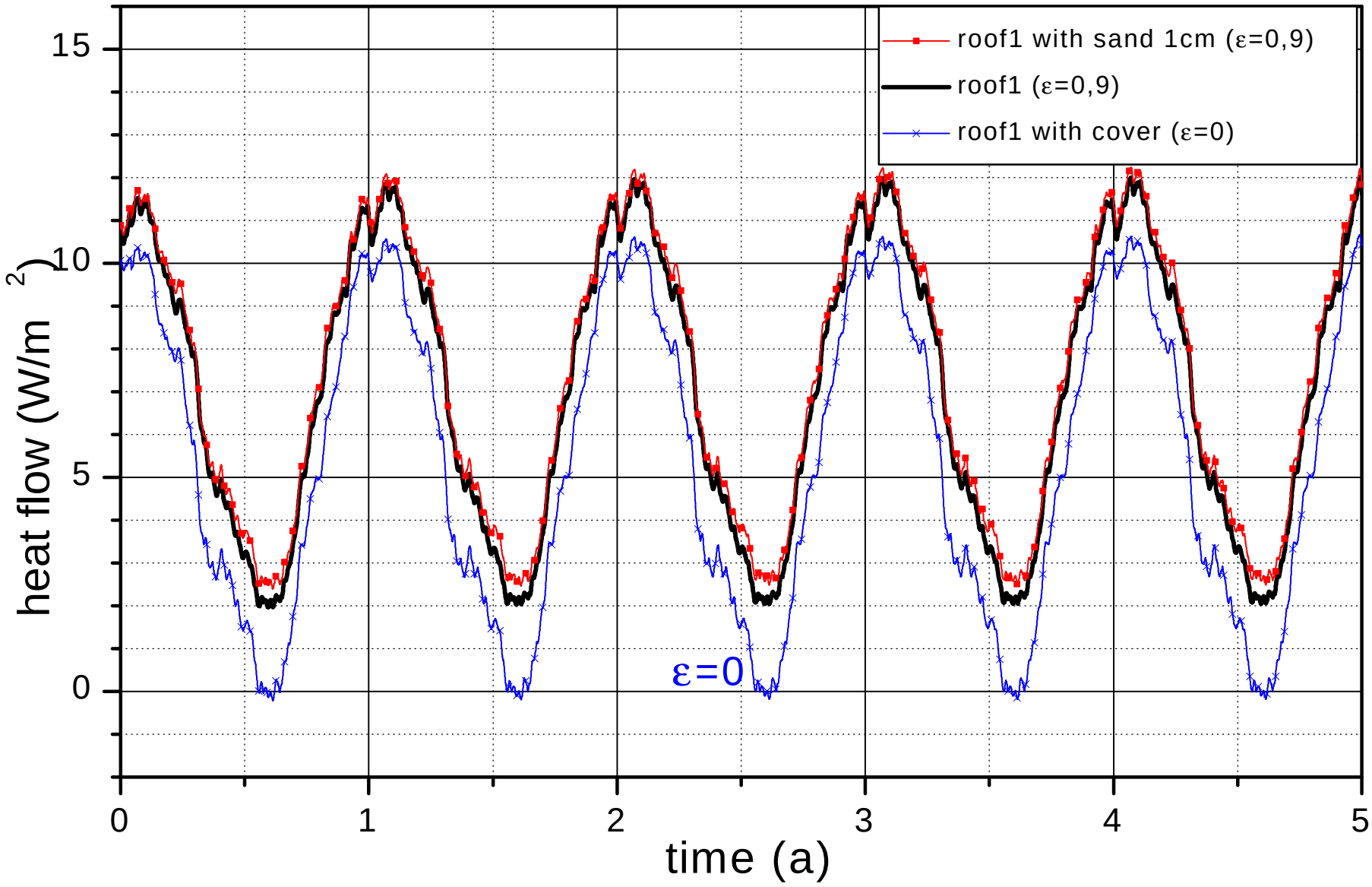

Fig.10 Heat flow density at the internal surface of a gas concrete flat roof structure, TRY Essen (roof 1).

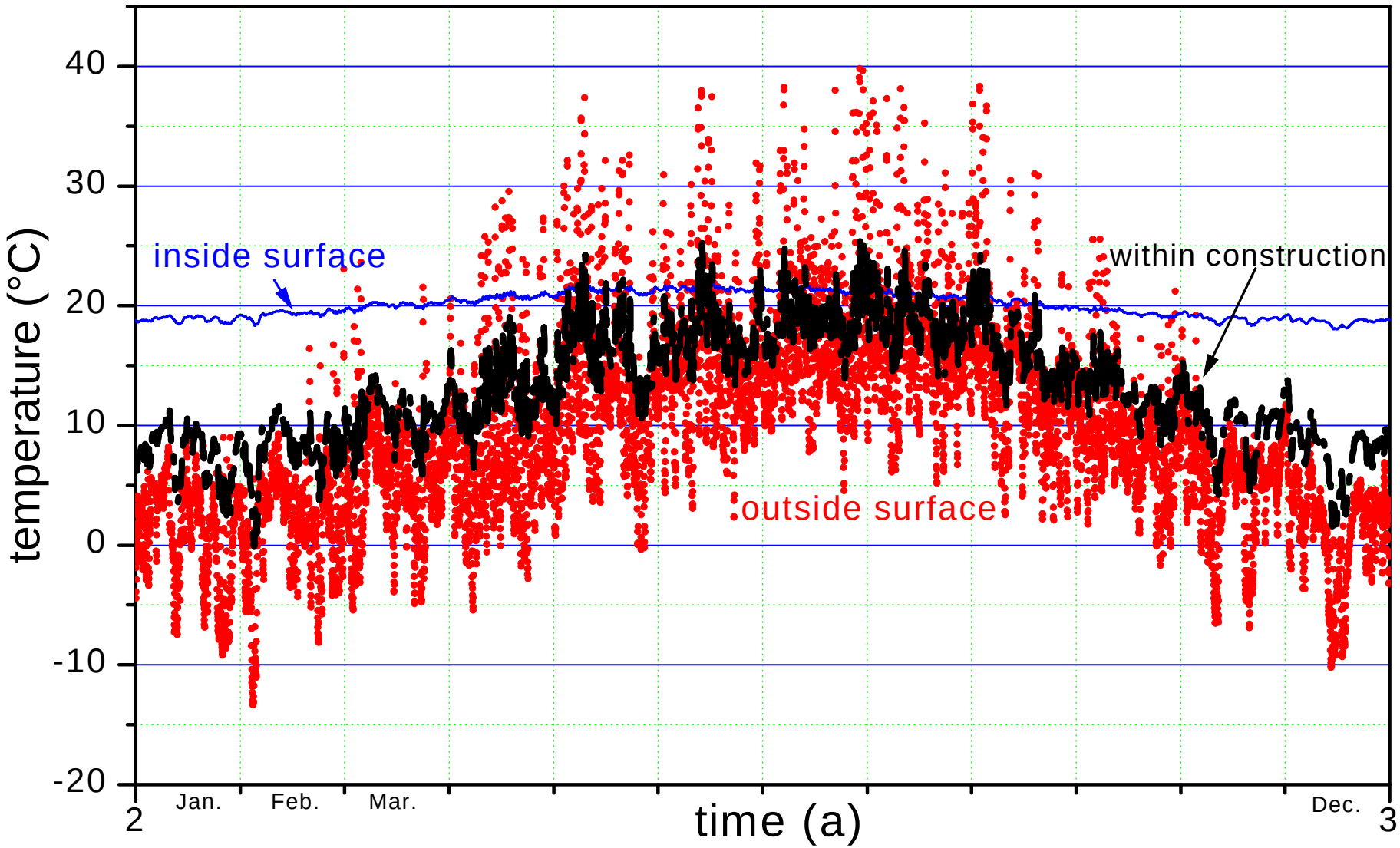

Fig.11 Course of temperature within and at the surface of a gas concrete flat roof structure, TRY Essen (roof 1).